Cancer Research

EGF816 Exerts Anticancer Effects in Non–Small Cell Lung Cancer by Irreversibly and Selectively Targeting Primary and Acquired Activating Mutations in the EGF Receptor

Yong Jia[1], Jose Juarez[1], Jie Li[1], Mari Manuia[1], Matthew J. Niederst[2], Celin Tompkins[1], Noelito Timple[1], Mei-Ting Vaillancourt[1], AnneMarie Culazzo Pferdekamper[1], Elizabeth L. Lockerman[2], Chun Li[1], Jennifer Anderson[1], Carlotta Costa[2], Debbie Liao[1], Eric Murphy[1], Michael DiDonato[1], Badry Bursulaya[1], Gerald Lelais[1], Jordi Barretina[3], Matthew McNeill[1], Robert Epple[1], Thomas H. Marsilje[1], Nuzhat Pathan[1], Jeffrey A. Engelman[2], Pierre-Yves Michellys[1], Peter McNamara[1], Jennifer Harris[1], Steven Bender[1], and Shailaja Kasibhatla[1]

Abstract

Non–small cell lung cancer patients carrying oncogenic EGFR mutations initially respond to EGFR-targeted therapy, but later elicit minimal response due to dose-limiting toxicities and acquired resistance. EGF816 is a novel, irreversible mutant-selective EGFR inhibitor that specifically targets EGFR-activating mutations arising *de novo* and upon resistance acquisition, while sparing wild-type (WT) EGFR. EGF816 potently inhibited the most common EGFR mutations L858R, Ex19del, and T790M *in vitro*, which translated into strong tumor regressions *in vivo* in several patient-derived xenograft models. Notably, EGF816 also demonstrated antitumor activity in an exon 20 insertion mutant model. At levels above efficacious doses, EGF816 treatment led to minimal inhibition of WT EGFR and was well tolerated. In single-dose studies, EGF816 provided sustained inhibition of EGFR phosphorylation, consistent with its ability for irreversible binding. Furthermore, combined treatment with EGF816 and INC280, a cMET inhibitor, resulted in durable antitumor efficacy in a xenograft model that initially developed resistance to first-generation EGFR inhibitors via cMET activation. Thus, we report the first preclinical characterization of EGF816 and provide the groundwork for its current evaluation in phase I/II clinical trials in patients harboring EGFR mutations, including T790M. *Cancer Res; 76(6); 1591–602. ©2016 AACR.*

Introduction

One of the major drivers in non–small cell lung cancer (NSCLC) is the EGFR proto-oncogene (1). The most common EGFR oncogenic mutations are either an amino acid substitution at position 858 from leucine (L) to arginine (R; L858R) or in-frame deletion within exon 19 (Ex19del). Together, these account for about 90% of all EGFR mutations (2). It is well established that lung cancers bearing these common mutations are highly responsive to first-generation EGFR inhibitors gefitinib and erlotinib with objective response rates of approximately 70% (3, 4). Common side effects of these drugs include skin rash, diarrhea, and loss of appetite, which are caused by inhibition of wild-type (WT) EGFR (5). In fact, skin rash has been suggested as a biomarker for drug efficacy (6). Unfortunately, drug resistance emerges in a majority of patients with a median time to progression of 9 to 12 months. In 50% of these cases, drug resistance is due to an amino acid substitution at gatekeeper position 790 from threonine (T) to methionine (M; T790M). The other 50% of drug resistance mechanisms involve signaling pathway activations bypassing EGFR such as MET amplification, epithelial–mesenchymal transition (EMT), SCLC transformation, or PI3K mutation (7, 8). In addition to being the predominant acquired mechanism of resistance, several groups have reported various rates of *de novo* T790M mutation in pretreatment specimens (9–12).

Second-generation EGFR inhibitor afatinib demonstrated improved activity against T790M-resistant models, but was also equally potent against WT EGFR, leading to a narrow safety window (13, 14). Accordingly, in clinical trials, the efficacy of afatinib in T790M-positive patients appeared to be constrained by the dose-limiting toxicities arising from WT EGFR inhibition (15).

Several experimental agents that overcome the T790M-driven resistance are now in clinical trials, including CO-1686 (16), AZD9291 (17), and EGF816 (ClinicalTrials.gov Identifier:

[1]Genomics Institute of the Novartis Research Foundation, San Diego, California. [2]Massachusetts General Hospital/Harvard Medical School Cancer Center, Charlestown, Massachusetts. [3]Novartis Institute for Biomedical Research, Cambridge, Massachusetts.

Note: Supplementary data for this article are available at Cancer Research Online (http://cancerres.aacrjournals.org/).

Corresponding Authors: Yong Jia, Genomics Institute of the Novartis Research Foundation, 10675 John J. Hopkins Dr., San Diego, CA 92121. Phone: 858-812-1728; Fax: 858-812-1918; E-mail: yjia@gnf.org; and Shailaja Kasibhatla, Phone: 858-332-4498; E-mail: skasibhatla@gnf.org

doi: 10.1158/0008-5472.CAN-15-2581

NCT02108964). All three agents are covalent EGFR inhibitors that are designed to selectively target the T790M mutation while sparing WT EGFR. Thus, the safety window with respect to EGFR inhibitor–associated side effects such as rash and diarrhea is expected to improve. During the review period of this article, AZD9291 (TAGRISSO) gained FDA-accelerated approval for treatment of EGFR T790M-positive lung cancer patients. The discovery of EGF816 will be disclosed elsewhere (18). Herein, we report the preclinical characterization of EGF816, and demonstrate its superior efficacy against primary activating and T790M-resistant mutations as well as its WT selectivity in comparison with early generation EGFR tyrosine kinase inhibitors (TKI) in various *in vitro* and *in vivo* models. In addition, we demonstrate that EGF816 is efficacious in exon 20 insertion (Ex20ins) mutants that are resistant to first-generation EGFR inhibitors.

Materials and Methods

Animals and cell lines

Female Foxn1 nude mice and rats were purchased from Harlan Laboratories and were between 6–8 or 5–10 weeks old, and 20–25 g or 150–230 g, respectively, at time of experiment. NOD.Cg-*Prkdc*^{scid} *Il2rg*^{tm1Wjl}/SzJ (NSG) mice were purchased from Jackson Laboratory and were between 6–8 weeks old and 20–25 g at time of experiment. All animal studies were conducted under a GNF Institutional Animal Care and Use Committee approved protocol in compliance with Animal Welfare Act regulations and the Guide for the Care and Use of Laboratory Animals. NCI-H1975, HCC827, NCI-H3255, and A431 were obtained from ATCC within the past 9 years. They were authenticated by Novartis department of Developmental and Molecular Pathways by SNP genotyping. HaCaT was kindly provided by K. Balavenkatraman from Novartis Basel. Human Epidermal Keratinocytes, neonatal (HEKn) were ordered from Invitrogen. Cells were routinely screened for *Mycoplasma sp*. by MycoAlert (Lonza) and used within a 4-month period from when they were thawed.

Cellular target modulation assays

H1975, H3255, HCC827, A431, and HaCaT cells were maintained in RPMI media supplemented with antibiotics and 10% FBS. HEKn cells were maintained in EpiLife media supplemented with growth supplement. All cells were maintained in a 37°C, 5% CO_2 humidified incubator. In 384-well plates, H1975, H3255, HCC827, A431, or HaCaT were seeded with RPMI media supplemented with antibiotics and 5% FBS, whereas HEKn cells were seeded in EpiLife media supplemented with 5% FBS. After an overnight incubation, serial diluted compounds were transferred to cells and incubated for 3 hours. HaCaT and HEKn cells were stimulated with 10 ng/mL EGF (50 ng/mL EGF for A431) for 5 minutes. Cells were lysed in 1% Triton X-100 buffer containing protease and phosphatase inhibitors. Lysates were analyzed by sandwich ELISA utilizing goat anti-EGFR capture antibody, anti-phospho-EGFR(Y1173), and anti-rabbit HRP. Signal was measured by chemiluminescent detection.

Receptor occupancy determination

Cells were labeled with ^{14}C-EGF816 for 3 hours in an incubator, washed with PBS, and lysed with 1% Triton X-100 buffer supplemented with protease inhibitors. Anti-EGFR sepharose was used for overnight immunoprecipitation. Beads were washed with lysis buffer and prepared for NuPAGE. Phosphor-imaging of dried gels was carried out with a Typhoon Phosphor Imager and EC_{50} values determined by graphical analysis.

Cellular proliferation assays

Cells were seeded 500 cells/well in solid white 384-well plates in maintenance media. Serial diluted compounds were transferred to cells. After 3 days, cell viability was measured by CellTiter-Glo (Promega) according to the manufacturer's instructions. BaF3 cell viability was measured 2 days after compound treatment using Bright-Glo Luciferase Assay System (Promega). Luminescent readout was normalized to 0.1% DMSO-treated cells and empty wells. Five EGFR TKI-resistant cell lines were generated at Massachusetts General Hospital (MGH, Boston, MA). MGH134, MGH121, MGH141, and MGH157 were derived from patients who developed resistance to erlotinib with acquired T790M mutation (19). MGH119-R was generated *in vitro* by treating MGH119 (EGFR Ex19del) with gefitinib for a prolonged period. The sensitivity of EGF816 on these lines was tested as described previously (20).

In vivo efficacy studies

H1975, HCC827, and H3255 cells were grown aseptically in a 37°C incubator with 5% CO_2. H1975 and H3255 were cultured in RPMI1640 media supplemented with 10% FBS and penicillin/streptomycin, 1 mmol/L sodium pyruvate, and 10 mmol/L HEPES. HCC827 was cultured in DMEM/F-12 media supplemented with 1.5 g/L sodium bicarbonate and 10% FBS.

For H1975 and HCC827 mouse tumor models, 5e6 or 10e6 cells, respectively, were subcutaneously implanted in female Foxn1 nude mice. For H3255 mouse tumor model, 5e6 cells were subcutaneously implanted in female NSG mice, and when tumors formed, fresh tumor tissues were implanted in female NSG mice. For H1975 rat tumor model, female Foxn1 nude rats received a single radiation dose of 400 to 500 rad 3 days before 5e6 cells were subcutaneously implanted. For LU0387 PDX model, tumor fragments from seed mice inoculated with primary human lung cancer tissues (LU0387) were harvested and used for inoculation into nude mice. Tumor volumes were measured by digital caliper three times a week and body weights of all animals were recorded throughout the study. Caliper measurements were calculated using $(L \times W^2)/2$.

EGF816 or afatinib were formulated in 0.5% methylcellulose (MC), 0.5% Tween80 suspension formulation. Erlotinib was formulated in 90% water, 10% ethanol/cremophor EL (1/1). Animals were weighed on dosing days and drugs were administered by oral gavage at 10 μL/g of body weight.

All data were expressed as mean ± SEM. Between-group comparisons were carried out in GraphPad Prism 6 using a one-way ANOVA followed by a *post hoc* Tukey or Dunn. The level of significance was set at $P < 0.05$. Significance compared with the vehicle control group is reported unless otherwise stated.

In vivo efficacy studies of EGF816 in two patient-derived xenograft models generated at MGH (MGH134 and MGH141) were conducted as described previously (20).

Pharmacodynamic measurement

Target inhibition of pEGFR, pAKT, and pERK *in vivo* was evaluated by either Western or Meso-Scale Discovery (MSD) technology. Western blot analyses of tumor sample lysates were

performed using standard techniques and included a 4°C overnight incubation with primary antibodies specific to the phosphorylated or total protein targets. Chemiluminescent signals were detected and quantified with the VersaDoc Imager (Bio-Rad). Phospho-EGFR band intensity was normalized to total EGFR band intensity for each tumor sample. In MSD-based assays, EGFR protein was captured using MSD Standard Streptavidin Gold plates (cat. no. L15AA-2, MSD) coated with 1 μg/mL of human EGFR biotinylated antibody (cat.no. BAF231, R&D Systems). Phospho-EGFR was detected with phospho-Tyr conjugated SULFO-TAG detection antibody (cat.no. R32AP-5, MSD). Data was calculated as percent of vehicle control.

Dusp6 expression measurement

Frozen skin from experimental rats was homogenized with TRIzol (Invitrogen) using the Qiagen TissueLyser. RNA was extracted following the manufacturer's specifications for the Qiagen RNeasy 96-well Universal Tissue kit, and quantified on the Nanodrop. cDNA was generated using the QuantiTect Whole Transcriptome Kit (Qiagen) and the high-yield 8-hour reaction. TaqMan qPCR was run using the RT2 kit (Qiagen) on the AB HT7900 machine according to the manufacturer's specifications. Samples were run in duplicate and normalized to Actin B.

WT pEGFR detection by IHC in normal skin tissues

Skin tissues from experimental mice were fixed in 10% neutral buffered formalin for 24 hours, then transferred to 70% ethanol. Tissues were processed into paraffin blocks and sectioned at 5 μm onto Superfrost Plus slides (Fisher). Slides were stained for pEGFR using the Ventana Discovery XT staining Module and a rabbit monoclonal antibody against Tyr1173. Additional background reducers were included (Dako).

Generation and characterization of EGF816-resistant *in vivo* models

Mice with stable HCC827 tumor (as described in the "*in vivo* efficacy studies" above) were dosed with EGF816 (10, 20, and 50 mg/kg escalated increasing) until tumor no longer responded to EGF816. The tumor became resistant to EGF816 after 103-day dosing. The fresh EGF816-resistant tumor tissues were implanted in SCID mice subcutaneously for efficacy study. EGF816 was formulated as described above. INC280 was formulated in 0.25% MC, 0.05% Tween 80 in water solution. Animals were weighed on dosing days and drugs were administered by oral gavage at 5 μL/g of body weight.

Additional Materials and Methods can be found in Supplemental Information.

Results

EGF816 is a potent inhibitor of mutant EGFR and shows good receptor occupancy in cells

EGF816 irreversibly targets EGFR by forming a covalent bond to C797 at the active site (Supplementary Fig. S1; ref. 18). The determined K_I and k_{inact} of EGF816 on EGFR(L858R/790M) mutant are 0.031 μmol/L and 0.222 min^{-1}, respectively.

The cellular activity of EGF816 on EGFR mutants were assessed using three well-characterized cell lines, H3255, HCC827, and H1975, which harbor the L858R, Ex19del, and L858R/T790M mutations, respectively. After incubation with cells for 3 hours, EGF816 showed potent inhibition of pEGFR levels in H3255, HCC827, and H1975 with EC_{50} values of 5, 1, and 3 nmol/L, respectively (Table 1; Fig. 1A). EGF816 was further evaluated for its ability to inhibit cell proliferation, where it produced EC_{50} values of 9, 11, and 25 nmol/L in H3255, HCC827, and H1975, respectively (Table 1; Fig. 1B). In contrast, erlotinib showed weak inhibitory effect on H1975 as expected, with EC_{50} values of 1,400 and 7,400 nmol/L in target modulation and proliferation assays, respectively (Fig. 1A and B). In addition, EGF816 was also tested in a panel of cell line models established directly from erlotinib-resistant patient biopsy samples that had acquired a T790M-resistant mutation. These cell lines were resistant to gefitinib; however, they were all sensitive to EGF816 treatment (Fig. 1C; Supplementary Table S1). As expected, EGF816 was also effective on the erlotinib-sensitive patient-derived cell line MGH119 (EGFR Ex19del mutation), but not on the WT EGFR-containing patient-derived cell lines MGH025 and NH11. Taken together, these data demonstrate that EGF816 is a potent inhibitor of cells driven by mutant EGFR.

The relationship between receptor occupancy and inhibition of signaling was investigated by exposing cells to ^{14}C-radiolabelled EGF816 for 3 hours, followed by quantification of the radiolabeled EGF816 by phosphor-imaging. As shown in Fig. 1D, a dose-dependent increase in signal until saturation was observed for H1975 and HCC827 cells, which indicated that EGF816 bound to mutant EGF receptors in a dose-dependent manner and was able to fully occupy the receptor at higher doses. Further data analysis showed that EGF816 has an OC_{50} (compound concentration at 50% occupancy) value of 2 and 5 nmol/L on HCC827 and H1975, respectively (Table 1; Fig. 1E), in a similar range as determined by ELISA-based target modulation assay (Table 1).

EGF816 induces tumor regression *in vivo* in several EGFR-mutant tumor models

EGF816 possesses favorable physicochemical properties and good oral bioavailability in mice (18). The antitumor activity

Table 1. Target modulation and antiproliferation EC_{50}, and receptor occupancy OC_{50} values of EGF816 on WT and mutant EGFR cell lines

Cell line	EGFR construct	Target modulation EC_{50} (nmol/L)	Receptor occupancy OC_{50} (nmol/L)	Proliferation EC_{50} (nmol/L)
H3255	L858R	5	ND	9
HCC827	Ex19del	1	2	11
H1975	L858R/T790M	3	5	25
HaCaT	WT	182	169	538
HEKn	WT	313	ND	ND
A431	WT	71	ND	4,994
BaF3/D770_N771insSVD	Ex20ins	ND	ND	7
BaF3/V769_D770insASV	Ex20ins	ND	ND	11
BaF3/H773_V774insNPH	Ex20ins	ND	ND	190
BaF3/WT EGFR	WT	ND	ND	166

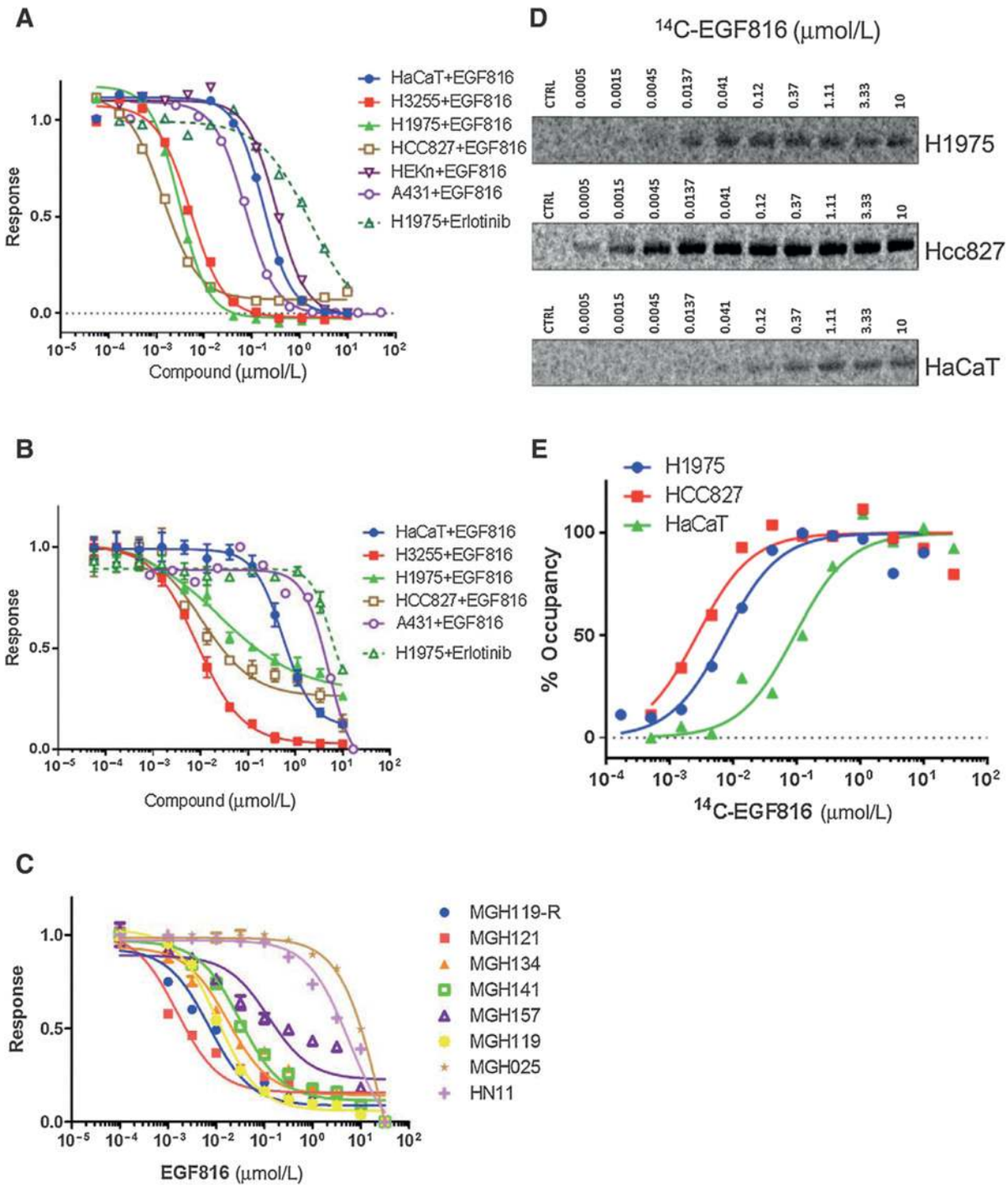

Figure 1.
Cellular activity of EGF816 in mutant and WT EGFR cell lines. A, target modulation EC_{50} of EGF816 in H3255 (L858R), HCC827 (Ex19del), H1975 (L858R/T790M), HaCaT (WT), HEKn (WT), and A431 (WT). "Response" is the relative phospho-EGFR level compared with DMSO. The effect of erlotinib on H1975 is shown as dotted line. B, antiproliferative EC_{50} of EGF816 in H3255, HCC827, H1975, HaCaT, and A431. "Response" is the relative luminescent signal compared with DMSO. The effect of erlotinib on H1975 is shown as dotted line. C, antiproliferative activity of EGF816 in a number of patient-derived cell lines obtained at MGH containing either mutant (MGH119-R_[Ex19del/T790M], MGH121_[Ex19del/T790M], MGH134_[L858R/T790M], MGH141_[Ex19del/T790M], MGH157_[Ex19del/T790M], and MGH119_[Ex19del]) or WT EGFR (MGH025 and HN1). "Response" is the relative signal compared with DMSO. D, phosphor-imaging of ^{14}C-labeled EGF816 on the EGF receptors. E, receptor occupancy OC_{50} of EGF816 on the EGF receptors determined by quantifying the phosphor-image of ^{14}C-labeled EGF816.

and tolerability of EGF816 was examined *in vivo* in several mutant EGFR-containing cell line xenograft models. In H1975 mouse model, oral administration of EGF816 once daily for 14 days resulted in dose-dependent efficacy (Fig. 2A). Although 3 mg/kg of EGF816 did not provide statistically significant efficacy compared with vehicle group ($P > 0.05$), EGF816 dosed at 10 mg/kg induced tumor growth inhibition with a T/C (tumor/control volume) of 29% ($P < 0.0001$). At higher doses of 30 and 100 mg/kg, significant tumor regressions (T/C, −61% and −80%, respectively) were achieved. Afatinib at 25 mg/kg showed a tumor growth inhibition corresponding to a T/C of 31%, similar to EGF816 at 10 mg/kg. Similar observations were obtained in the H1975 rat xenograft model (Fig. 2B). Fourteen days after treatment, tumor growth was significantly inhibited (T/C of 11%) at 10 mg/kg. Partial to complete tumor regressions (T/C, −78% and −100%, respectively) were achieved at 30 and 100 mg/kg of EGF816. Afatinib showed a tumor growth inhibition corresponding to T/C of 56% at 10 mg/kg. The lowest tested dose of EGF816 at 10 mg/kg was more efficacious and significantly different from afatinib at 10 mg/kg ($P < 0.0001$) in this model.

In the HCC827 mouse xenograft model, the lowest oral dose of 3 mg/kg once daily for 21 days induced statistically significant tumor regression (T/C of −74%; Fig. 2C). Near complete regression with T/C of −92%, −96%, and −98% was observed at EGF816 doses of 10, 30, and 100 mg/kg. As expected, the HCC827 model was also sensitive to erlotinib, which at 30 and 60 mg/kg achieved regressions similar to that of EGF816 at 3 mg/kg (Fig. 2C). Erlotinib at its MTD of 120 mg/kg showed similar maximum efficacy as EGF816 at 10 mg/kg or above. In the H3255 xenograft model, oral dosing of EGF816 at 30 mg/kg once daily achieved significant antitumor activity compared with vehicle ($P < 0.0001$), and resulted in a tumor regression of 85% (Fig. 2D). In a separate study in the same model, once daily oral dosing of erlotinib at 100 mg/kg achieved 82% tumor regression. In addition, EGF816 was tested in xenograft models generated from patient-derived cell lines MGH134 (L858R/T790M) and MGH141 (Ex19del/T790M). Both patients developed T790M resistance following erlotinib treatment in the clinic. In both models, treatment with EGF816 at 30 mg/kg induced significant tumor regression (Fig. 2E and F).

Compound tolerability was monitored by group percent body weight change as shown in Supplementary Fig. S2. EGF816 was well tolerated, and body weights were maintained at all doses during the course of treatment. However, afatinib showed slight body weight loss (∼5%) at 25 mg/kg once daily (Supplementary Fig. S2A), a dose that also resulted in tumor growth inhibition corresponding to T/C of 31% (Fig. 2A). Erlotinib was also tolerated at lower doses of 30 and 60 mg/kg, but at MTD of 120 mg/kg, moderate body weight loss (∼12% on day 11) was observed (Supplementary Fig. S2B). In all the models tested, EGF816 demonstrated an improved therapeutic index compared with the earlier generation EGFR inhibitors.

EGF816 inhibits EGFR and downstream signaling pathways *in vivo*

To confirm the *in vivo* efficacy of EGF816 was due to its ability to effectively suppress EGFR signaling, a single-dose experiment was conducted in both H1975 and HCC827 mouse xenograft models to examine the kinetics of target inhibition by EGF816 with respect to plasma exposure. Following a single dose of EGF816, a time course of pathway inhibition was determined by Western blotting of tumor lysates. In both models, there was a dose-dependent increase in both the extent and duration of pEGFR inhibition (Fig. 3A, Supplementary Fig. S3A). In the H1975 model, at 3 and 10 mg/kg, the pEGFR levels were inhibited partially within the 24-hour period. At 30 mg/kg, the dose that gave significant tumor regression in the 14-day efficacy study (Fig. 2A), inhibition of pEGFR was observed as early as 1-hour postdose and was maintained through 24 hours with >80% inhibition. Levels of pEGFR returned to baseline at 48-hour postdose (Fig. 3A). In addition, downstream biomarkers such as pAKT and pERK were also inhibited as early as 1-hour postdose and maintained for ≥7-hour postdose, and returned to baseline levels at 16- to 24-hour postdose (Fig. 3B). In the HCC827 model, at 1 mg/kg, the pEGFR level was inhibited partially within the 24-hour period, but at 3 and 10 mg/kg, the doses that gave significant tumor regression in the 14-day efficacy study (Fig. 2C), pEGFR levels were inhibited for >80% within the 24-hour period (Supplementary Fig. S3A). Inhibition of pEGFR and downstream biomarkers such as pAKT and pERK was observed as early as 1-hour postdose and was maintained through 24-hour post-single oral dose of EGF816 at 10 mg/kg (Supplementary Fig. S3B). In both models, total EGFR, AKT, and ERK protein levels were not affected by EGF816.

Together, these data suggest that sustained high level inhibition of pEGFR is required for good antitumor efficacy in mouse xenograft models. In both models, pEGFR inhibition outlasted pharmacokinetics, which was consistent with the irreversible binding mechanism of action of EGF816. The HCC827 model was more sensitive to EGF816 with higher and more sustained inhibition at the same dose level than the H1975 model. This was supported by pharmacokinetic/pharmacodynamic modeling, which showed that pEGFR protein synthesis rate is approximately five times faster in the H1975 xenograft model than in the HCC827 model (unpublished observations).

EGF816 is selective against WT EGFR

To demonstrate the selectivity of EGF816 toward mutant forms of EGFR, multiple approaches were taken. First, we determined the binding affinity of EGF816 to a panel of kinases, where it showed high-affinity binding to 16/451 kinases (Supplementary Fig. S4). These included mutant forms of EGFR as well as nine kinases with an analogous Cys residue at a similar location in the active site as EGFR. To evaluate the selectivity of EGF816 on mutant over WT EGFR, we employed three different WT EGFR cell line models: A431, HEKn, and HaCaT. The epidermoid carcinoma cell line A431 contains amplified EGFR (21); alternatively, the spontaneously immortalized keratinocyte cell line (HaCaT) and primary keratinocytes (HEKn) contain nonamplified EGFR levels, and their dependence on ErbB signaling for proliferation or survival has been described previously (22, 23). We believe these two lines serve as better models than A431 in studying skin toxicity due to WT EGFR inhibition. Regardless of which WT cell line model was used, cellular-based assays showed that EGF816 is selective toward mutant over WT EGFR (Table 1). In patient-derived cell line models, EGF816 selectively targeted EGFR-mutant–containing lines over WT EGFR lines (Supplementary Table S1). Furthermore, profiling of 89 lung cancer models showed that EGF816 is selective against EGFR-mutant cell lines (whose mutations are within catalytic domain) compared with WT

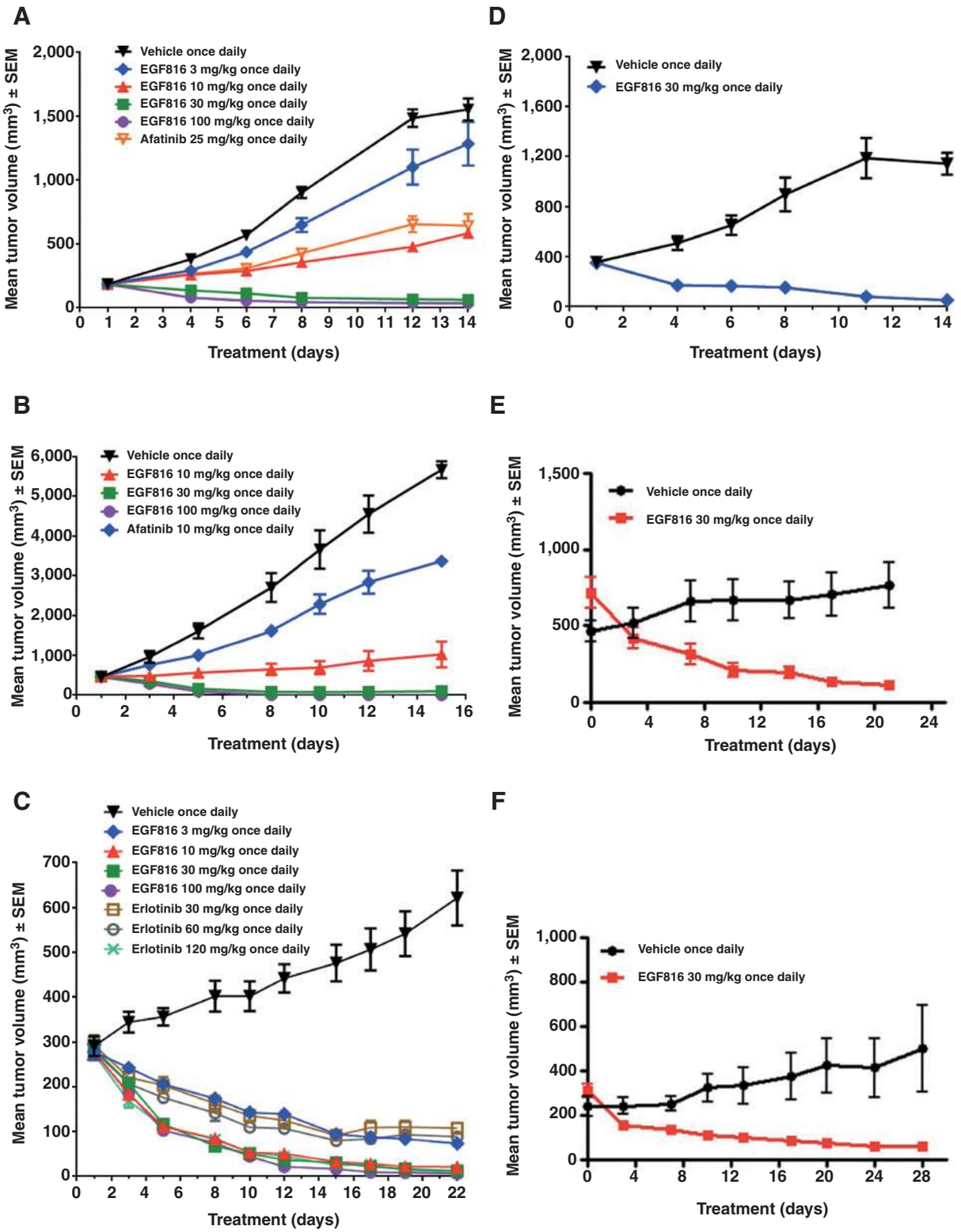

Figure 2.
In vivo efficacy of EGF816 in EGFR-mutant–containing cell line xenograft models following 14 days (A, B, D) or 21 days (C, E, F) of once daily oral dosing. A, EGF816 and afatinib in H1975 (EGFR L858R/T790M) mouse xenograft model. B, EGF816 and afatinib in H1975 (EGFR L858R/T790M) rat xenograft model. C, EGF816 and erlotinib in HCC827 (EGFR Ex19del) mouse xenograft model. D, EGF816 in H3255 (EGFR L858R) mouse xenograft model. E, EGF816 in MGH134 (EGFR L858R/T790M) mouse xenograft model. F, EGF816 in MGH141 (EGFR Ex19del/T790M) mouse xenograft model.

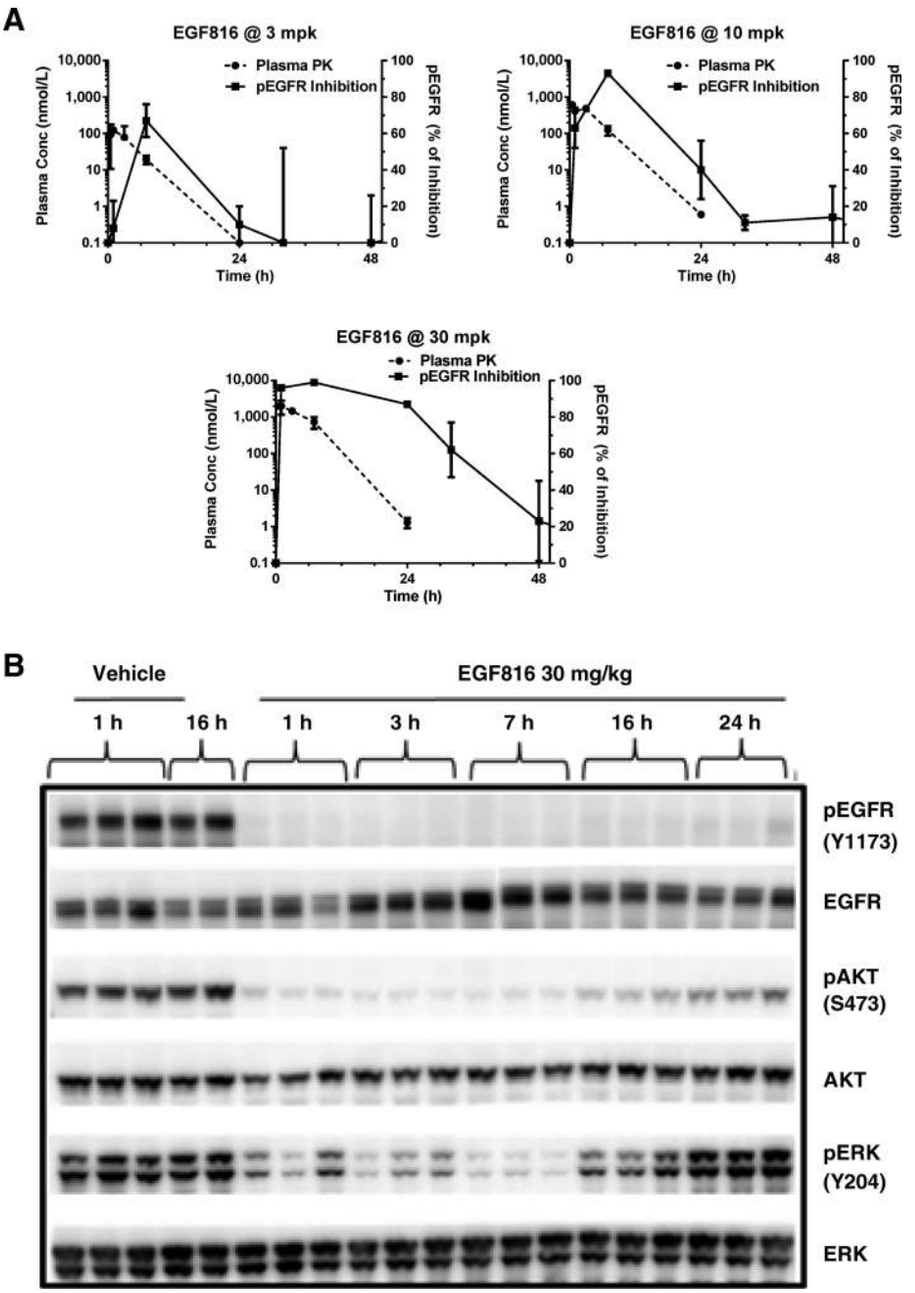

Figure 3.
EGF816 inhibits EGFR phosphorylation and downstream signaling pathways *in vivo* in H1975 (EGFR L858R/T790M) mouse xenograft model. A, time course of pEGFR inhibition in relation to plasma pharmacokinetics of EGF816 after single oral dose of EGF816 at 3, 10, and 30 mg/kg. EGF816 shows both dose-dependent and time-dependent inhibition of pEGFR. B, time course of pEGFR and downstream signal markers pAKT and pERK inhibition by Western blotting following single oral dose of EGF816 at 30 mg/kg.

EGFR lines (Fig. 4A) with the only exception of NCI-H1650 (24). However, NCI-H1650 has been reported to be resistant to EGFR inhibition due to PTEN loss (25).

Inhibition of EGFR in cells generally decreases the expression level of dual specificity phosphatase 6 (Dusp6) via inhibition of the MAPK pathway (26, 27). Consequently, the effect on Dups6 expression in normal skin may be one way to assess the WT EGFR selectivity of EGF816. In the H1975 rat xenograft model, Dusp6 gene expression was measured in rat skin after 14 days of once daily dosing (Fig. 4B). EGF816 at efficacious doses of 10 and 30 mg/kg (Fig. 2B) did not appear to inhibit Dusp6 expression in rat skin, whereas afatinib at 10 mg/kg (significantly less efficacious; Fig. 2B) caused significant inhibition of Dusp6 expression (~80% inhibition). EGF816 at the highest dose of 100 mg/kg inhibited the Dusp6 gene expression by approximately 70%, consistent with a large but finite *in vivo* selectivity of EGF816 for mutant versus WT EGFR.

Furthermore, the effect of EGF816 on WT EGFR phosphorylation *in vivo* was assessed directly. Phospho-EGFR levels were determined by IHC in normal mouse skin tissues taken from HCC827 efficacy studies after 21 days of dosing (Fig. 4C). Even at 100 mg/kg dose, which is fully efficacious (Fig. 2C), pEGFR level in normal tissue is comparable with that of vehicle control, which

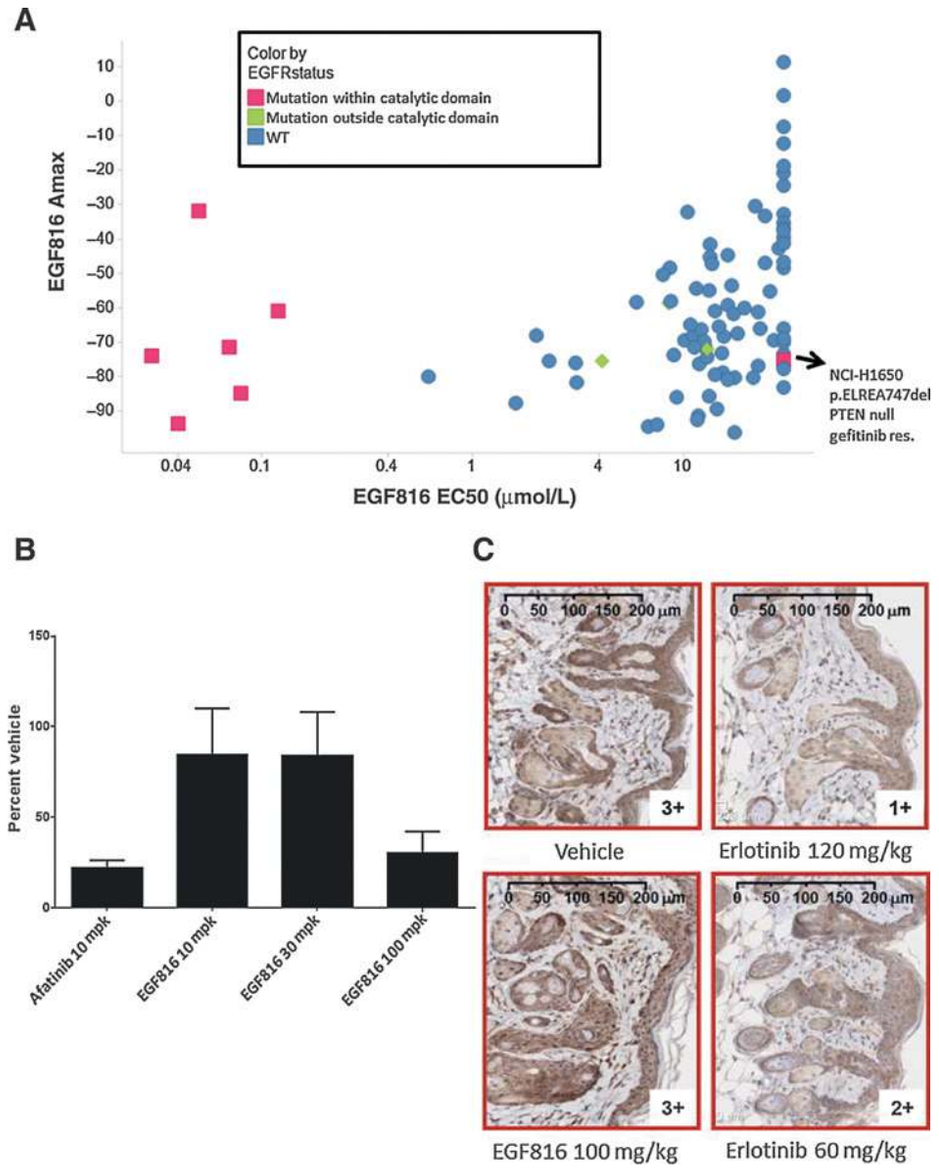

Figure 4.
EGF816 selectively targets mutant EGFR versus WT EGFR. A, antiproliferative activity of EGF816 on 89 lung cancer cell lines indicated that EGF816 selectively inhibited cell lines containing EGFR with catalytic domain mutations. B, change in relative Dusp6 expression levels in rat skin following 14 days of once daily oral dosing of EGF816 and afatinib in H1975 tumor bearing nude rats. EGF816 inhibited Dusp6 expression only at highest does of 100 mg/kg, whereas lower doses of EGF816 had no effect. In contrast, afatinib at less efficacious dose of 10 mg/kg showed significant inhibition of Dusp6 expression. C, IHC staining of WT pEGFR in normal mice skin from HCC827 efficacy studies dosed with EGF816 and erlotinib. Even at 100 mg/kg dose, EGF816 showed no significant effect on WT EGFR phosphorylation. In contrast, erlotinib showed significant and dose-dependent inhibition of WT pEGFR.

indicated minimal WT EGFR inhibition by EGF816. On the contrary, erlotinib showed dose-dependent inhibition of WT EGFR as expected.

All together, these results strongly indicate that EGF816 possesses good selectivity for mutant EGFR compared with WT EGFR.

EGF816 is efficacious in an exon 20 insertion mutant model *in vivo*

Ex20ins mutation is the third largest EGFR-mutant population, consisting of 4% to 9% of all EGFR-mutant NSCLC (28). These insertion mutations occur in multiple forms (base pair insertions and/or duplications) as well as at multiple codons in exon 20 (predominately clustered between codons 763–774). On the basis of preclinical studies and clinical observations, all Ex20ins mutants (except A763_Y764insFQEA), for the most part, are associated with lower sensitivity to clinically achievable doses of current EGFR TKIs, including third-generation inhibitors AZD9291 and CO-1686 (16, 17, 29–32). To understand whether EGF816 had any efficacy against this class of EGFR mutants, we chose three Ex20ins mutants of highest clinical frequency, and generated engineered BaF3 cell lines: D770_N771insSVD, V769_D770insASV, and H773_V774insNPH (29). In the proliferation-based assays, EGF816 potently inhibited these three Ex20ins mutants, with EC_{50} of 7, 11, and 190 nmol/L on D770_N771insSVD, V769_D770insASV, and H773_V774insNPH, respectively (Table 1). This promising result prompted us to test the antitumor effect of EGF816 in an EGFR Ex20ins PDX model (LU0387; H773_V774insNPH). Oral administration of EGF816 at 30 mg/kg once daily for 18 days achieved 45% tumor inhibition. EGF816 at 100 mg/kg resulted in a tumor regression of 81% and achieved significant antitumor activity compared with vehicle ($P < 0.0001$; Fig. 5A). Both doses were well tolerated (Fig. 5B). These results suggest that EGF816

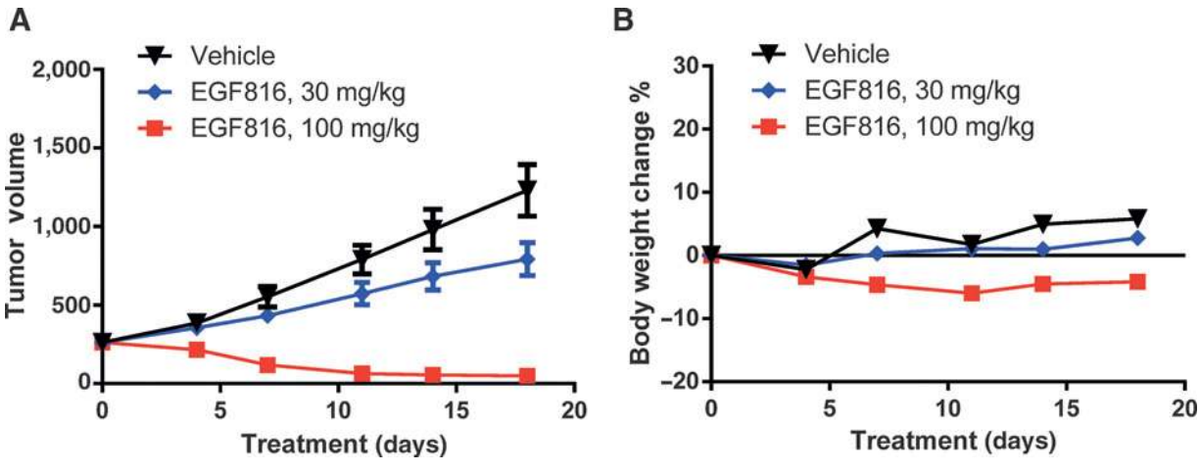

Figure 5.
In vivo antitumor efficacy (A) and tolerability (B) of EGF816 in LU0387 (EGFR Ex20_H773_V774insNPH) mouse PDX model following 18 days of once daily oral dosing.

might be efficacious in patients harboring exon20 insertion mutations and that its use in this patient population merits further investigation in the clinic.

C797S mutation, MET amplification, and EMT are among the mechanisms of acquired resistance to EGF816 in preclinical models

Acquired resistance to EGF816 was studied in cellular models using two different methods. In the BaF3-based rapid mutagenesis approach, EGFR L858R and L858R/T790M BaF3 lines were randomly mutated by treatment with ENU (N-ethyl-N-nitrosourea). Selection pressure was applied with EGF816 from 80 to 1,000 nmol/L gradually over a period of 1 month. Deep sequencing identified several hot spot mutations that led to resistance to EGF816, one of the highest frequency mutations being C797S. This same mutation was also reported by Janne and colleagues following a similar approach using another irreversible EGFR inhibitor WZ-4002 (33). Cys797 is the amino acid that is covalently modified by irreversible EGFR inhibitors. The mutation of this residue to Ser abolishes the covalent interaction of the inhibitor with the EGFR protein, thus greatly reducing the affinity/potency of these irreversible inhibitors. In a different approach where resistance to EGF816 was generated by stepwise method, H1975 and HCC827 cell lines were treated with increasing concentrations of EGF816 from IC_{30} to 1,000 nmol/L (>IC_{90}) over a period of approximately 6 months. A total of 11 and 6 resistant clones were isolated and further characterized from EGF816-resistant H1975 and HCC827, respectively. None of these resistant clones showed reactivation of pEGFR, suggesting that resistance is due to other pathway activations that bypass EGFR signaling (Fig. 6A). Instead, we observed EMT in 9/11 and 2/6 resistant clones of H1975 and HCC827, respectively (Fig. 6A). The induction of EMT protein marker expression correlated with changes in morphology (Supplementary Fig. S5). It was further confirmed that all of the EGF816 resistant clones were also resistant to other available EGFR inhibitors.

Using the *in vivo* mouse models of H1975 and HCC827, an attempt to generate acquired resistance to EGF816 was performed by continuously treating the animals with either fixed (H1975) or incrementally higher (HCC827) doses of EGF816. H1975 resistance did not occur even after 3 months of continuous dosing at 30 mg/kg EGF816. In HCC827, however, resistance to EGF816 emerged in about 2 months. Phospho-RTK array analysis revealed MET pathway activation (Fig. 6B). Single-agent treatment of a reimplanted, resistant tumor with either EGF816 or selective cMET inhibitor INC280 (34) resulted in mild tumor growth inhibition (difference between the two groups is not statistically significant; Fig. 6C). Only the dual inhibition of EGFR and cMET with EGF816/INC280 combination induced significant and durable tumor regression.

Discussion

Targeted therapies have changed the landscape of cancer treatment. NSCLC patients with oncogenic EGFR mutations are one patient population benefiting considerably from targeted therapies (35). Earlier generations of EGFR inhibitors have revolutionized the treatment of NSCLC and are effective in treating patients with oncogenic mutations L858R and Ex19del. However, dose-limited toxicities due to WT EGFR inhibition and eventual acquired resistance have limited their use. Third-generation EGFR inhibitors have the potential to overcome these limitations and improve the treatment options for patients who have progressed because of resistance. AZD9291 and CO-1686 are third-generation covalent EGFR inhibitors with distinct profiles over the earlier generation inhibitors; they inhibit both activating and resistant EGFR mutations with selectivity over WT EGFR. As demonstrated in this article, EGF816 is another novel third-generation EGFR inhibitor that potently inhibits activating (L858R, Ex19del) and resistant T790M mutants with nanomolar potency in various cellular assays (Table 1). In addition, EGF816 also potently inhibits a panel of patient-derived cell lines that harbor Ex19del, L858R/T790M, or Ex19del/T790M mutations (Supplementary Table S1). Taking advantage of its covalent binding, the receptor occupancy of EGF816 was directly visualized using radiolabeled compound. Our data show that EGF816 is able to fully

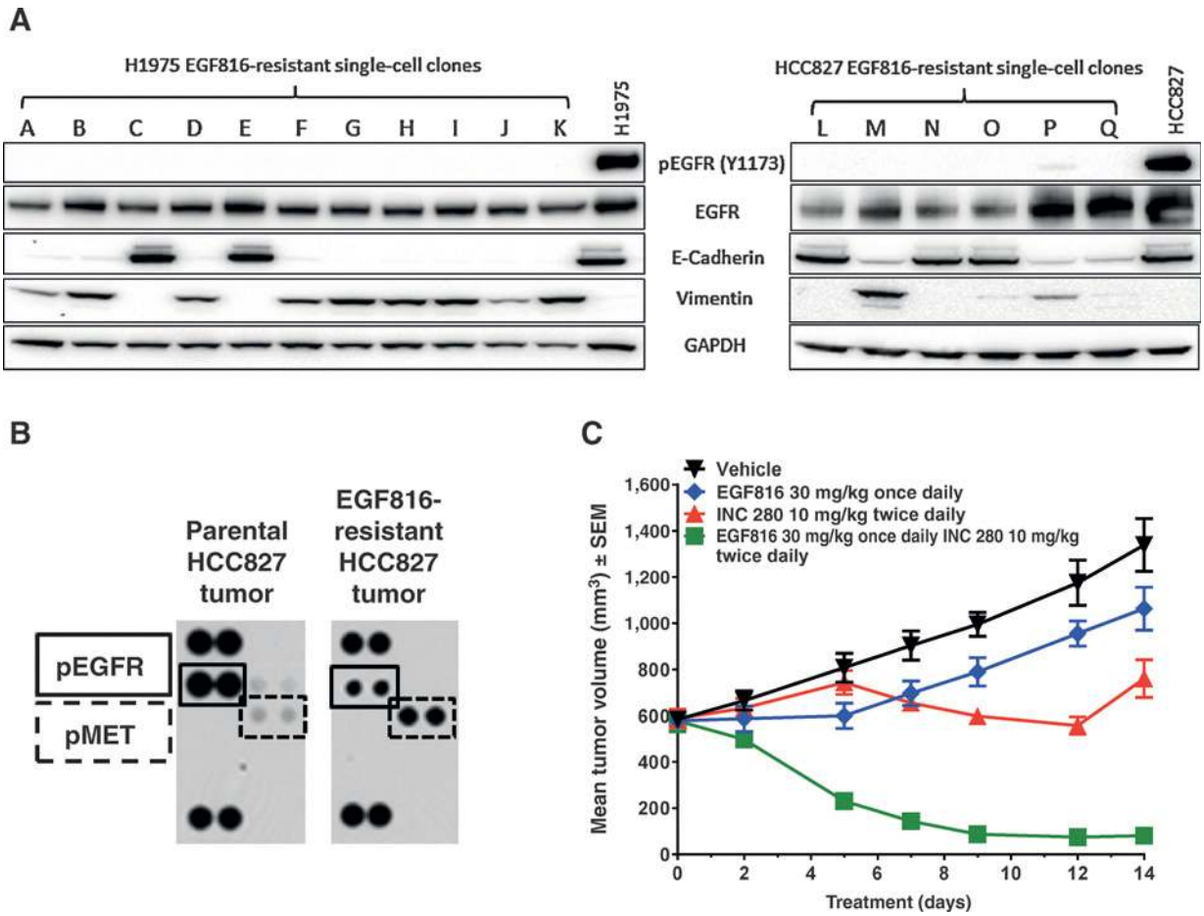

Figure 6.
Acquired resistance to EGF816 in preclinical models. A, Western blot analysis of EGF816-resistant single-cell–derived clones in H1975 (clone A–K) and HCC827 (clone L–Q). pEGFR signal was abolished in all clones, indicating resistance occurred through other mechanisms bypassing EGFR signaling. Clone A, B, D, F–K, M, and P showed EMT signature. B, phospho-RTK array analysis of tumor lysates from parental and EGF816-resistant HCC827 tumor showed cMET activation in the EGF816-resistant tumor. C, *in vivo* efficacy in EGF816-resistant HCC827 mouse xenograft model following 14 days of oral dosing of either EGF816 (30 mg/kg, once daily) or INC280 (10 mg/kg, twice daily), or combination of the two agents.

occupy (inhibit) mutant EGFRs at exposures achievable *in vivo* (Fig. 1D). This is significant as EGFR is upstream of signaling cascades, so complete and sustained inhibition is likely required to totally shut down the downstream signaling and promote cell-cycle arrest and apoptosis. This is supported by our observation in the *in vivo* pharmacodynamic/efficacy correlation studies where sustained high level of pEGFR inhibition is required for good antitumor efficacy in mouse xenograft models. Covalent inhibitors are an excellent choice as they possess the properties of good potency and can lead to sustained target inhibition, where extent and duration of target modulation are determined by target protein synthesis rate, inactivation efficiency of inhibitor, and inhibitor concentration. EGF816 has a longer half-life in human than mouse. In phase I trial, at all doses tested in human, exposures achieved were above the targeted exposure required for tumor regression predicted by xenograft model. Pharmacokinetic/pharmacodynamic and pharmacokinetic/efficacy relationship and modeling, as well as clinical findings will be published elsewhere.

Even though H1975 is the most widely used patient-derived cell line model for EGFR L858R/T790M, we also conducted an efficacy study in the L858R/T790M-driven patient-derived xenograft model MGH134. The results are in good agreement with those obtained in H1975 model. Marked tumor regressions were also observed following treatment of mice bearing MGH141 (Ex19del/T790M) patient-derived xenograft. Our *in vivo* data revealed that EGF816 outcompeted earlier generation EGFR inhibitors with superior efficacy and improved therapeutic index. Although irreversible mutant-selective EGFR inhibitors such as EGF816 were originally designed to overcome the T790M resistance, their target profiles suggest that they present an alternative and better therapy option for both oncogenic and resistant T790M mutations as first-line therapy.

WT EGFR plays an important role in normal tissues, including skin (36). Patients treated with early generation EGFR inhibitors can develop a papulopustular rash, dry skin, itching, and hair and periungual alterations, resulting in decreased quality of life (37). One of the hallmarks of mutant-selective EGFR inhibitors is that

they have improved WT EGFR selectivity, thus are expected to be better tolerated. We took several approaches to evaluate the WT EGFR selectivity of EGF816. When profiled against a large panel of lung cancer cell lines *in vitro*, EGF816 showed excellent selectivity on mutant versus WT EGFR containing cell lines. We further examined WT EGFR inhibition *in vivo* by either indirectly measuring the WT EGFR biomarker Dusp6 expression in rat skin or directly measuring WT EGFR phosphorylation in mouse skin. Both sets of data demonstrated that EGF816 minimally affected WT EGFR *in vivo* at efficacious doses. On the basis of these data, we expect EGF816 to be well tolerated in human with respect to WT EGFR–related toxicities.

Besides the commonly occurring activating (L858R, Ex19del) and T790M-resistant mutations, the third largest EGFR-mutant population in NSCLC is Ex20ins mutations (28). It has been reported that, in the most part, currently approved EGFR TKIs are ineffective on activating Ex20ins mutations based on preclinical studies (16, 17, 29), thus presenting an urgent unmet medical need. To our surprise, EGF816 showed potent *in vitro* antiproliferative effects in three Ex20ins mutant cell lines tested, and induced near full tumor regression in one patient-derived Ex20ins xenograft model *in vivo* at a well-tolerated dose. At this time, it is not clear whether the differential effect of EGF816 versus AZD9291/CO-1686 in Ex20ins mutant models is compound specific or model specific. Both AstraZeneca and Clovis used Ex20_H773_V774HVdup model, which has very rare clinical incidence (16, 17, 29). On the other hand, the models we tested have the highest clinical incidence, where the three Ex20ins mutants studied accounted for approximately 47% of the Ex20ins mutant population. At 100 mg/kg dosing where tumor regression was observed in the LU0387 model, WT EGFR inhibition was also observed (Fig. 4B). Therefore, the therapeutic window for Ex20_H773_V774insNPH might be smaller than that for activating EGFR mutations. However, on the basis of *in vitro* cell line results, EGF816 is much more potent on Ex20_D770_N771insSVD and Ex20_V769_D770insASV mutants than Ex20_H773_V774insNPH (Table 1). Unfortunately, we could not determine the *in vivo* efficacy of EGF816 in Ex20_D770_N771insSVD and Ex20_V769_D770insASV due to lack of PDX models. If a correlation does exist between the *in vitro* and *in vivo* results, we would expect EGF816 to be efficacious in the Ex20_D770_N771insSVD and Ex20_V769_D770insASV models *in vivo* at lower doses, thus creating a larger therapeutic window.

Despite the potential of third-generation EGFR inhibitors to inhibit and prevent T790M-mediated acquired resistance, tumors will likely adapt other escape mechanisms to develop resistance. Understanding potential resistance mechanisms using preclinical models is therefore important and could guide combination therapies to overcome resistance. Similar to our observations, EMT seems to be the major resistance mechanism for CO-1686 in preclinical models (16). Resistance to third-generation EGFR inhibitors is now starting to emerge in the clinic. Clovis reported that WT-EGFR clone outgrowth due to tumor heterogeneity plays a major role in CO-1686 resistance (38). AstraZeneca reported C797S mutation as one of the resistance mechanisms to AZD9291 (39). The same C797S mutation was found in MGH121 cells made resistant *in vitro* to a third-generation EGFR inhibitor (40). In addition, MET amplification was also seen as a resistance mechanism to CO-1686 in the clinic (41). It is encouraging to see the translation of preclinical observations into clinical findings. Further preclinical investigation is beneficial to design strategies to prevent and/or overcome acquired resistance using rational combination therapies. In the ongoing clinical trial treating gefitinib-resistant patients due to MET activation, the combination of INC280 and gefitinib seems promising (42). Planned clinical trials of EGF816 combination therapies include INC280 and will help us better understand the clinical benefit of this approach (ClinicalTrials.gov Identifier: NCT02335944)

EGF816 is currently being evaluated in phase I/II clinical trials in patients harboring EGFR mutations, including T790M.

Disclosure of Potential Conflicts of Interest

M.J. Niederst is a consultant/advisory board member for Boehringer Ingelheim. J.A. Engelman reports receiving commercial research grants from Novartis (sponsored research agreement through MGH) and AstraZeneca (sponsored research agreement through MGH); has ownership interest (including patents) in Gatekeeper; and is a consultant/advisory board member for AstraZeneca, Clovis, Novartis, and Roche/Genentech. No potential conflicts of interest were disclosed by the other authors.

Authors' Contributions

Conception and design: Y. Jia, G. Lelais, J. Barretina, M. McNeill, R. Epple, T.H. Marsilje, N. Pathan, P.-Y. Michellys, P. McNamara, J. Harris, S. Bender, S. Kasibhatla

Development of methodology: Y. Jia, J. Juarez, J. Li, M. Manuia, C. Tompkins, J. Anderson, E. Murphy, M. McNeill, N. Pathan, J. Harris, S. Kasibhatla

Acquisition of data (provided animals, acquired and managed patients, provided facilities, etc.): J. Juarez, J. Li, M. Manuia, M.J. Niederst, C. Tompkins, N. Timple, M.-T. Vaillancourt, A.M.C. Pferdekamper, C. Li, J. Anderson, C. Costa, J. Barretina, M. McNeill, N. Pathan, J.A. Engelman, S. Kasibhatla

Analysis and interpretation of data (e.g., statistical analysis, biostatistics, computational analysis): Y. Jia, J. Juarez, J. Li, M. Manuia, M.J. Niederst, C. Tompkins, N. Timple, M.-T. Vaillancourt, A.M.C. Pferdekamper, C. Li, D. Liao, E. Murphy, B. Bursulaya, J. Barretina, M. McNeill, R. Epple, N. Pathan, S. Kasibhatla

Writing, review, and/or revision of the manuscript: Y. Jia, J. Juarez, M. Manuia, N. Timple, M.-T. Vaillancourt, A.M.C. Pferdekamper, C. Li, G. Lelais, J. Barretina, M. McNeill, P. McNamara, S. Bender, S. Kasibhatla

Administrative, technical, or material support (i.e., reporting or organizing data, constructing databases): Y. Jia, J. Juarez, J. Li, C. Tompkins, E.L. Lockerman

Study supervision: Y. Jia, E. Murphy, J. Barretina, N. Pathan, J.A. Engelman, S. Kasibhatla

Other (provided structural biology support for the development of EGF816): M. DiDonato

The costs of publication of this article were defrayed in part by the payment of page charges. This article must therefore be hereby marked *advertisement* in accordance with 18 U.S.C. Section 1734 solely to indicate this fact.

Received September 21, 2015; revised December 31, 2015; accepted January 1, 2016; published OnlineFirst January 29, 2016.

References

1. The Cancer Genome Atlas Research Network. Comprehensive molecular profiling of lung adenocarcinoma. Nature 2014;511:543–50.
2. Sharma SV, Bell DW, Settleman J, Haber DA. Epidermal growth factor receptor mutations in lung cancer. Nat Rev Cancer 2007;7:169–81.
3. Lynch TJ, Bell DW, Sordella R, Gurubhagavatula S, Okimoto RA, Brannigan BW, et al. Activating mutations in the epidermal growth factor receptor underlying responsiveness of non–small-cell lung cancer to gefitinib. N Engl J Med 2004;350:2129–39.

4. Paez JG, Jänne PA, Lee JC, Tracy S, Greulich H, Gabriel S, et al. EGFR mutations in lung cancer: correlation with clinical response to gefitinib therapy. Science 2004;304:1497–500.
5. Herbst RS, LoRusso PM, Purdom M, Ward D. Dermatologic side effects associated with gefitinib therapy: clinical experience and management. Clin Lung Cancer 2003;4:366–9.
6. Dienstmann R, Braña I, Rodon J, Tabern J. Toxicity as a biomarker of efficacy of molecular targeted therapies: focus on EGFR and VEGF inhibiting anticancer drugs. Oncologist 2011;16:1729–40.
7. Sequist LV, Waltman BA, Dias-Santagata D, Digumarthy S, Turke AB, Fidias P, et al. Genotypic and histological evolution of lung cancers acquiring resistance to EGFR inhibitors. Sci Transl Med 2011;3:75ra26.
8. Pao W, Miller VA, Politi KA, Riely GJ, Somwar R, Zakowski MF, et al. Acquired resistance of lung adenocarcinomas to gefitinib or erlotinib is associated with a second mutation in the EGFR kinase domain. PLoS Med 2005;2:e73.
9. Inukai M, Toyooka S, Ito S, Asano H, Ichihara S, Soh J, et al. Presence of epidermal growth factor receptor gene T790M mutation as a minor clone in non–small cell lung cancer. Cancer Res 2006;66:7854–8.
10. Su K, Chen H, Li K, Kuo M, Yang JC, Chan W, et al. Pretreatment epidermal growth factor receptor (EGFR) T790M mutation predicts shorter EGFR tyrosine kinase inhibitor response duration in patients with non–small-cell lung cancer. J Clin Oncol 2012;30:433–40.
11. Rosell R, Molina MA, Costa C, Simonetti S, Gimenez-Capitan A, Bertran-Alamillo J, et al. Pretreatment EGFR T790M mutation and BRCA1 mRNA expression in erlotinib-treated advanced non-small-cell lung cancer patients with EGFR mutations. Clin Cancer Res 2011;17:1160–8.
12. Maheswaran S, Sequist LV, Nagrath S, Ulkus L, Brannigan B, Collura CV, et al. Detection of mutations in EGFR in circulating lung-cancer cells. N Engl J Med 2008;359:366–77.
13. Li D, Ambrogio L, Shimamura T, Kubo S, Takahashi M, Chirieac LR, et al. BIBW2992, an irreversible EGFR/HER2 inhibitor highly effective in preclinical lung cancer models. Oncogene 2008;27:4702–11.
14. Schwartz PA, Kuzmic P, Solowiej J, Bergqvist S, Bolanos B, Almaden C, et al. Covalent EGFR inhibitor analysis reveals importance of reversible interactions to potency and mechanisms of drug resistance. Proc Natl Acad Sci U S A 2014;111:173–8.
15. Yu HA, Pan W. Afatinib—new therapy option for EGFR-mutant lung cancer. Nat Rev Clin Oncol 2013;10:551–2.
16. Walter AO, Sjin RT, Haringsma HJ, Ohashi K, Sun J, Lee K, et al. Discovery of a mutant-selective covalent inhibitor of EGFR that overcomes T790M-mediated resistance in NSCLC. Cancer Discov 2013;3:1404–15.
17. Cross DA, Ashton SE, Ghiorghiu S, Eberlein C, Nebhan CA, Spitzler PJ, et al. AZD9291, an irreversible EGFR TKI, overcomes T790M-mediated resistance to EGFR inhibitors in lung cancer. Cancer Discov 2014;4:1046–61.
18. Lelais G, Epple R, Marsilje TH, Long YO, McNeill M, Chen B, et al. Discovery of a novel and potent mutant selective EGFR inhibitor (EGF816) for the treatment of EGFR mutant non-small cell lung cancers. J Med Chem 2016. Manuscript in revision.
19. Niederst MJ, Sequist LV, Poirier JT, Mermel CH, Lockerman EL, Garcia AR, et al. RB loss in resistant EGFR mutant lung adenocarcinomas that transform to small-cell lung cancer. Nat Commun 2015;6:6377.
20. Crystal AS, Shaw AT, Sequist LV, Friboulet L, Niederst MJ, Lockerman EL, et al. Patient-derived models of acquired resistance can identify effective drug combinations for cancer. Science 2014;346:1480–6.
21. Merlino GT, Xu YH, Ishii S, Clark AJ, Semba K, Toyoshima K, et al. Amplification and enhanced expression of the epidermal growth factor receptor gene in A431 human carcinoma cells. Science 1984;224:417–9.
22. Stoll SW, Benedict M, Mitra R, Hiniker A, Elder JT, Nuñez G. EGF receptor signaling inhibits keratinocyte apoptosis: evidence for mediation by Bcl-XL. Oncogene 1998;16:1493–9.
23. Peus D, Hamacher L, Pittelkow MR. EGF-receptor tyrosine kinase inhibition induces keratinocyte growth arrest and terminal differentiation. J Invest Dermatol 1997;109:751–6.
24. Barretina J, Caponigro G, Stransky N, Venkatesan K, Margolin AA, Kim S, et al. The cancer cell line encyclopedia enables predictive modelling of anticancer drug sensitivity. Nature 2012;483:603–7.
25. Sos ML, Koker M, Weir BA, Heynck S, Rabinovsky R, Zander T, et al. PTEN loss contributes to erlotinib resistance in EGFR-mutant lung cancer by activation of Akt and EGFR. Cancer Res 2009;69:3256–61.
26. Vecchione L, Jacobs B, Normanno N, Ciardiello F, Tejpar S. EGFR-targeted therapy. Exp Cell Res 2011;317:2765–71.
27. Caunt CJ, Keyse SM. Dual-specificity MAP kinase phosphatases (MKPs): shaping the outcome of MAP kinase signaling. FEBS J 2013;280:489–504.
28. Arcila ME, Nafa K, Chaft JE, Rekhtman N, Lau C, Reva BA, et al. EGFR exon 20 insertion mutations in lung adenocarcinomas: prevalence, molecular heterogeneity, and clinicopathologic characteristics. Mol Cancer Ther 2013;12:220–9.
29. Yasuda H, Kobayashi S, Costa DB. EGFR exon 20 insertion mutations in non-small-cell lung cancer: preclinical data and clinical implications. Lancet Oncol 2012;13:e23–31.
30. Yasuda H, Park E, Yun CH, Sng NJ, Lucena-Araujo AR, Yeo WL, et al. Structural, biochemical, and clinical characterization of epidermal growth factor receptor (EGFR) exon 20 insertion mutations in lung cancer. Sci Transl Med 2013;5:216ra177.
31. Greulich H, Chen TH, Feng W, Janne PA, Alvarez JV, Zappaterra M, et al. Oncogenic transformation by inhibitor-sensitive and -resistant EGFR mutants. PLoS Med 2005;2:e313.
32. Voon PJ, Tsui DWY, Rosenfeld N, Chin TM. EGFR exon 20 insertion A763-Y764insFQEA and response to erlotinib – Letter. Mol Cancer Ther 2013;12:2614–5.
33. Ercan D, Choi HG, Yun C-H, Capelletti M, Xie T, Eck MJ, et al. EGFR mutations and resistance to Irreversible pyrimidine based EGFR inhibitors. Clin Cancer Res 2015;21:3913–23
34. Liu X, Wang Q, Yang G, Marando C, Koblish HK, Hall LM, et al. A novel kinase inhibitor, INCB28060, blocks c-MET-dependent signaling, neoplastic activities, and cross-talk with EGFR and HER-3. Clin Cancer Res 2011;17:7127–38.
35. Cagle PT, Chirieac LR. Advances in treatment of lung cancer with targeted therapy. Arch Pathol Lab Med 2012;136:504–9.
36. Jost M, Kari C, Rodeck U. The EGF receptor — an essential regulator of multiple epidermal functions. Eur J Dermatol 2000;10:505–10.
37. Lacouture ME. Mechanisms of cutaneous toxicities to EGFR inhibitors. Nat Rev Cancer 2006;6:803–12.
38. Piotrowska Z, Niederst MJ, Karlovich CA, Wakelee HA, Neal JW, Mino-Kenudson M. Heterogeneity underlies the emergence of EGFR T790 wild-type clones following treatment of T790M-positive cancers with a third generation EGFR inhibitor. Cancer Discov 2015;5:713–22.
39. Thress KS, Paweletz CP, Felip E, Cho BC, Stetson D, Dougherty B, et al. Acquired EGFR C797S mutation mediates resistance to AZD9291 in non–small cell lung cancer harboring EGFR T790M. Nat Med 2015;21:560–2.
40. Niederst MJ, Hu H, Mulvey HE, Lockerman EL, Garcia AR, Piotrowska Z, et al. The allelic context of the C797S mutation acquired upon treatment with third generation EGF inhibitors impacts sensitivity to subsequent treatment strategies. Clin Cancer Res 2015;21:3924–33.
41. Haringsma HJ, Allen A, Harding TC, Simmons AD. *In vivo* acquired resistance to the mutant EGFR inhibitor rociletinib (CO-1686) is associated with activation of the c-MET pathway [abstract]. In: Proceedings of the 106th Annual Meeting of the American Association for Cancer Research; 2015 Apr 18–22; Philadelphia, PA. Philadelphia (PA): AACR; 2015. P3595. Abstract nr 3595.
42. Wu Y-L, Yang JC, Kim D-W, Su W-C, Ahn M-J, Lee DH, et al. Safety and efficacy of INC280 in combination with gefitinib (gef) in patients with EGFR-mutated (mut), MET-positive NSCLC: a single-arm phase Ib/II study. J Clin Oncol 32:5s, 2014 (suppl; abstr 8017).